Journal of Biochemistry and Molecular Biology, Vol. 33, No. 3, May 2000, pp. 268-275

JOURNAL OF
Biochemistry
and
Molecular Biology

Structure of a DNA Duplex Containing a Site-Specific Dewar Isomer: Structural Influence of the 3'-T·G base pair of the Dewar product.

Joon-Hwa Lee and Byong-Seok Choi*

Department of Chemistry and School of Molecular Science, Korea Advanced Institute of Science and Technology, 373-1, Kusong-dong, Yusong-gu, Taejon 305-701, Korea

Received 3 March 2000, Accepted 18 April 2000

In contrast to the pyrimidine (6-4)pyrimidone photoproduct [(6-4) adduct], its Dewar valence isomer (Dewar product) is low mutagenic and produces a broad range of mutations with a 42% replicating error frequency. In order to determine the origin of the mutagenic property of the Dewar product, we used experimental NMR restraints and molecular dynamics to determine the solution structure of a Dewar-lesion DNA decamer duplex, which contains a mismatched base pair between the 3'-T residue and an opposed G residue. The 3'-T of the Dewar lesion forms stable hydrogen bonds with the opposite G residue. The helical bending and unwinding angles of the DW/GA duplex, however, are much higher than those of the DW/AA duplex. The stable hydrogen bonding of the G15 residue does not increase the thermal stability of the overall helix. It also does not restore the distorted backbone conformation of the DNA helix that is caused by the forming of a Dewar lesion. These structural features implicate that no thermal stability, or conformational benefits of G over A opposite the 3'-T of the Dewar lesion, facilitate the preferential incorporation of an A. This is in accordance with the A rule during translesion replication and leads to the low frequent 3'-T→C mutation at this site.

Keywords: Dewar product, DNA damage, Mutagenesis, NMR, Solution structure.

Introduction

UV light irradiation of DNA produces a variety of photoproducts that strongly block DNA replication (Brash, 1988; Mitchell, 1988). When a SOS response is induced, these photoproducts are bypassed with modest efficiency by the DNA polymerase and give rise to mutations (Banerjee *et al.*, 1988; LeClerc *et al.*, 1991). This process was termed translesion replication (TR), or bypass synthesis, and was caused by the tendency of DNA polymerase to insert an incorrect nucleotide opposite the lesion during TR (Fuchs & Napolitano, 1998; Tomer *et al.*, 1998). Although both the (6-4) adduct, which is one of the major classes of UV-induced DNA photoproducts (Mitchell & Nairn, 1989; Pfeifer, 1997), and its Dewar valence isomer (Dewar product) (Figure 1A) cause mutations during TR, their mutagenic properties are contrasting. The (6-4) adduct is highly mutagenic and yields a specific mutation (LeClerc *et al.*, 1991; Smith *et al.*, 1996). In SOS-induced *Escherichia coli* cells, the marked preference for the insertion of G opposite the 3'-T of (6-4) adducts during TR leads to a predominant 3'-T→C transition with 85% replicating error frequency (LeClerc *et al.*, 1991). The Dewar product though is less mutagenic and induces a broader range of mutations than the (6-4) adduct (LeClerc *et al.*, 1991; Smith *et al.*, 1996). In SOS-induced *E. coli* cells, adenine was found to be incorporated into the site opposite the 3'-T of the Dewar product with a frequency of 72%; whereas, G was incorporated only 21% of the time (LeClerc *et al.*, 1991). In results, the 3' T→C transition, the major class of mutations

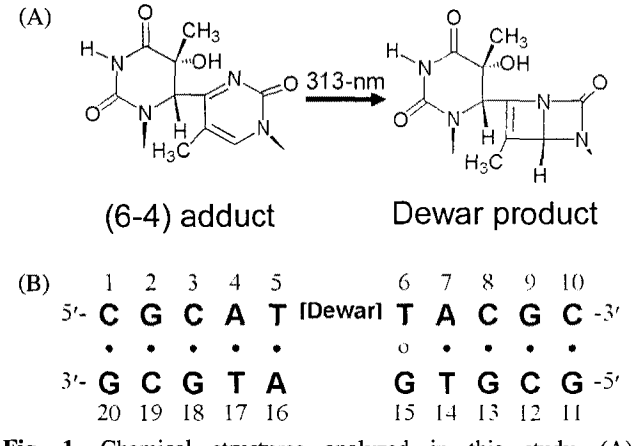

Fig. 1. Chemical structures analyzed in this study. (A) Chemical structures of the (6-4) adduct and the Dewar product. (B) DNA sequence context of the DW/GA duplex.

*To whom correspondence should be addressed.
Tel: 82-42-869-2828; Fax: 82-42-869-2810
E-mail: bschoi@cais.kaist.ac.kr

induced by the Dewar product, is produced with 13% replicating error frequency during TR (LeClerc *et al.*, 1991).

The nucleotide substitution mutations, which that are induced by the DNA lesions during the TR result from the misinstructive or noninstructive properties of the distorted templates. Opposite the abasic site (the prototypical noninstructional DNA lesion), an A residue is incorporated with a frequency of 77% during TR in *E. coli* (Jiang & Taylor, 1993). This preferential incorporation of an A residue opposite an abasic lesion with a low specificity is referred to as the "A rule" (Sagher & Strauss, 1983). NMR studies suggested that the A opposite abasic site stacks better in a intrahelical configuration than other bases and causes no helical distortion (Cuniasse *et al.*, 1987; Kalnik *et al.*, 1988). The term "misinstructive" is used to indicate the existence of the physical interactions between a distorted template and an incoming dNTP (Banerjee *et al.*, 1991). It has been reported that the (6-4) adduct is a misinstructional DNA lesion and the 3' T→C transition that is induced by the (6-4) adduct is caused by important physical features, such as hydrogen bonding, high thermal stability, and no backbone distortion (Lee *et al.*, 1999). The thermodynamics study has shown that the ΔG° value of the DNA helix containing the 3'-T·G base pair of the (6-4) adduct is much lower than that for the 3'-T·A base pair. The difference, however, for the Dewar product is very small (Fujiwara & Iwai, 1997). This result may partially explain the differences in the mutagenic properties of the two photoproducts, but it is still not sufficient to understand why the Dewar product would be less lethal than the (6-4) adduct. In order to completely understand the preferential insertion of the A residue at the 3'-T site of the Dewar lesion, you need a structural study of a DNA duplex containing a Dewar product in a mutated sequence context.

In this report, the conformational influence of the 3'-T·G base pair in the DNA decamer duplex, which contains a mismatched base pair between the 3'-T of the Dewar product and an opposed G residue [designated by the DW/GA duplex, Figure 1B], has been compared in detail with that of the 3'-T·A base pair in the DW/AA duplex. This was established in our previous work (Lee *et al.*, 1998). This structural comparison provides insight into the mechanism that determines the base selection during TR and can account for the origin of the mutagenic property of the Dewar product.

Materials and Methods

Sample preparation The single-stranded oligonucleotides, d(CGCATTACGC) and d(GCGTGAT GCG) were synthesized by the phosphoramidite method on a DNA synthesizer (Applied Biosystem, model 391). The crude 5'-dimethoxytritilated oligonucleotides were deprotected by treatment with concentrated ammonia for 12 hours at 55°C. The DNA products were purified by reverse-phase HPLC and desalted by Sephadex G-25 column (Lee *et al.*, 1997; Park *et al.*, 1998).

The thymine (6-4) adduct was produced by irradiating the oligonucleotide, d(CGCATTACGC), in a aqueous solution contained in large petri dish using a radiation reactor (New Southern England UV Products, model RPR-2000) equipped with twelve 35 W germicidal lamps (254 nm) for 6 hours. The average irradiating intensity was 80 J/m^{2}s. The temperature of the reactor chamber was maintained around 10°C by purging with liquid nitrogen gas during irradiation. Irradiated samples were dried and fractionated using a preparative μ-Bondapak C-18 HPLC column with a 60 min 10-20% methanol gradient in a 20 mM sodium phosphate buffer, pH 7.0, at a flow rate of 2.5 ml/min. The (6-4) adduct, which was characterized by a maximum absorption band at near 325 nm, was repurified by HPLC with a 60 min 10-20% methanol gradient in the previous buffer system and by Sephadex G-25 column. The (6-4) adduct, containing a DNA decamer duplex, was prepared by dissolving the lesion that contained the complementary oligonucleotide strand (adjusted to a stoichiometric 1 : 1 ratio), an aqueous solution containing a 10 mM sodium phosphate (pH 6.6) and 200 mM NaCl. Photoisomerization of the (6-4) adduct to its Dewar valence isomer in the duplex was performed by direct UV irradiation with 313 nm wavelength in the NMR tube. Complete conversion was confirmed by observing the significant disappearance of the T6-H6 resonance and the upfield shift of the T6-methyl resonance in the ^{1}H-NMR experiment.

NMR experiments All NMR experiments were carried out using Bruker DMX-600 spectrometers. The data were processed using a Silicon Graphics workstation with the program *XWIN* and *FELIX 95.0*. The spectra were recorded within the temperature range of 1-25°C. For observation of the exchangeable protons, one-dimensional proton spectra in a H_2O solution were collected with water suppression by a jump-and-return pulse. The NOESY spectrum in the H_2O solution at 1°C was recorded using the jump-and-return pulse sequence for the reading pulse. The phase-sensitive NOESY spectra in the D_2O solution were recorded using time-proportional phase incrementation at 1°C. The spectra were acquired with 2 K data-points in the t_2 dimension and 512 points in the t_1 dimension. The time-domain data were zero-filled in both directions to 4K54K and multiplied with a phase-shifted squared-sine function before Fourier transformation. NOE distance restraints from nonexchangeable protons were obtained from 2D-NOESY experiments with mixing times of 50, 80, 160, and 300 ms in a D_2O buffer solution. Exchangeable proton NOEs were determined using NOESY spectra in H_2O buffer with 120 and 400 ms mixing times. Watson-Crick-type hydrogen bonding restraints were imposed in each base pair, except the T5·A16 and T6·G15 base pairs.

Structure calculation The structure of the DW/GA duplex was calculated using the program *X-PLOR 3.1* (Brünger, 1992) with restrained molecular dynamics (RMD). We initially generated the normal A- and B-form starting structures with the modification of the Dewar product at the T5-T6 position. These structures were subjected to the RMD and simulated annealing (SA) protocol. The first stage of computation began with energy minimization, followed by 10 ps of MD at 1000 K. The force constants for the distance restraints were gradually increased over 10 cycles of 1 ps dynamics. The final values of the force constants were 100 kcal/molÅ^2. The system was subsequently cooled to 300 K over 10

cycles of 0.5 ps dynamics followed by energy minimization. The final stage involved 20 ps of the RMD at 300 K, and the structures were subsequently energy minimized. Fourteen structures (7 of the B-form and 7 of the A-form initial structures) were chosen on the basis of the lowest NOE violations and total energies.

The mean structure of the RMD-refined structures was then optimized using full relaxation matrix refinement (based on NOE intensity) with *X-PLOR*. NOE volumes from 738 cross peaks of the three mixing times of 50, 80, and 160 ms were used as restraints. The first stage of computation began with 10 ps of MD at 500 K. The force constants for the distance restraints were gradually decreased to zero and those of the intensity restraints were increased to 100 kcal/mol over 10 cycles of 0.5 ps dynamics. The system was subsequently cooled to 300 K over 5 cycles of 0.5 ps dynamics followed by energy minimization. The final stage involved 10 ps of the MD at 300 K, and the structures were subsequently energy minimized. Eight structures were chosen on the basis of the lowest total energies. The helical parameters of the refined structures were calculated using the program *CURVES*.

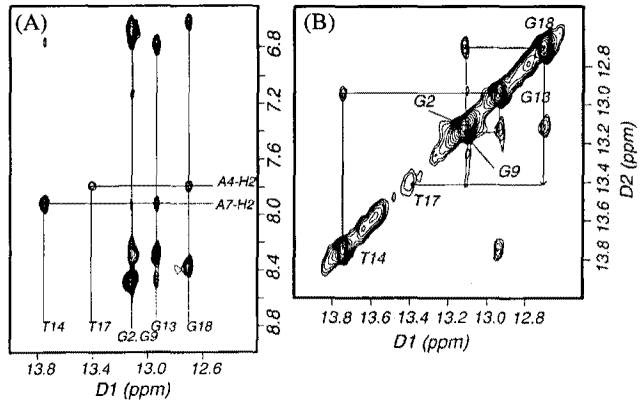

Fig. 2. Expanded NOESY (120-ms) contour plots of the DW/GA duplex in H_2O buffer solution (A) NOE cross peaks between the G-imino and C-amino protons of the G C base pairs and those between T-imino and A-H2 protons of the T A base pairs. (B) Sequential connectivity between imino protons of the (n)- and ($n+1$)-base pairs.

Results and Discussion

Resonance assignment of the exchangeable protons The one- and two-dimensional NMR data on the DW/GA duplex in the H_2O solution were analyzed to elicit the base pairing and stacking in the vicinity of the Dewar lesion. The NOESY spectra of the DW/GA duplex is shown in Figure 2, in which all imino protons were assigned following the standard analysis scheme of labile protons. The H5 protons of all C residues exhibited NOEs to both the hydrogen-bonded and non-hydrogen-bonded amino protons. One amino proton of each C residue also exhibited an NOE to the other amino proton. The imino protons of all G C base pairs were assigned by observing a set of NOE cross peaks from the C amino protons, which were assigned by intraresidue NOEs of H5↔H_2 to the G imino proton on the opposed base (Figure 2A). The imino protons of all T A base pairs were assigned from NOEs between the T imino protons and the H2 protons on the opposite A residue. The H2 protons of adenine residues were assigned from intraresidue NOEs of H2↔1'. The imino

Table 1. Chemical shifts of proton resonances in the DW/GA duplex.

Base	NH/NH_2	H2/H5/Me	H6/H8	H1'	H2'/H2"	H3'	H4'
C1	7.18/8.27	5.93	7.68	5.78	2.05/2.46	4.76	4.12
G2	13.16	-	8.01	5.93	2.761	5.03	4.42
C3	6.66/8.41	5.48	7.40	5.73	2.14/2.45	4.89	4.28
A4	-	7.83	8.36	6.35	2.78/2.88	4.99	4.43
T5	na[2]	0.95	4.39	5.97	2.08/2.45	4.43	4.00
T6	-	1.78	4.75	5.31	2.08/2.18	4.75	3.99
A7	-	7.96	8.54	6.30	2.84/2.95	5.07	4.48
C8	6.82/8.32	5.40	7.36	5.63	2.03/2.37	4.87	4.19
G9	13.14	-	7.92	6.00	2.63/2.77	5.02	4.42
C10	6.72/8.33	5.34	7.42	6.19	2.25/2.66	4.56	4.06
G11	13.10	-	8.03	6.03	2.71/2.84	4.92	4.34
C12	6.69/8.52	5.43	7.48	5.81	2.23/2.52	4.96	4.26
G13	12.97	-	8.02	6.02	2.69/2.82	5.05	4.44
T14	13.79	1.52	7.10	5.94	1.85/2.37	4.87	4.26
G15	10.24	-	7.92	5.44	2.31/2.44	5.00	4.17
A16	-	7.69	8.29	6.13	2.71/2.77	5.01	4.38
T17	13.44	1.35	7.21	5.74	2.19/2.40	4.89	4.16
G18	12.74	-	7.95	5.95	2.70/2.73	5.03	4.43
C19	6.74/8.52	5.48	7.43	5.85	2.01/2.42	4.90	4.26
G20	13.25	-	8.02	6.21	2.42/2.70	4.75	4.25

[1]Overlapped. [2]Not assigned.

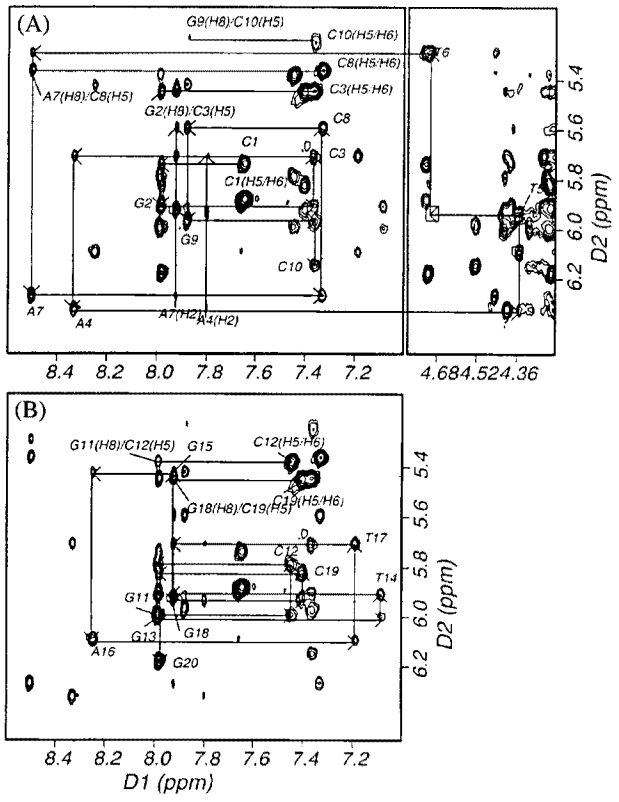

Fig. 3. Temperature dependence of the imino proton resonances of the ^{1}H-NMR spectra for the DW/GA duplex in an H_2O buffer solution. The positions of nucleotides in the decamer duplex that give rise to the resonances are indicated. The experimental temperatures are shown at the right of the figure.

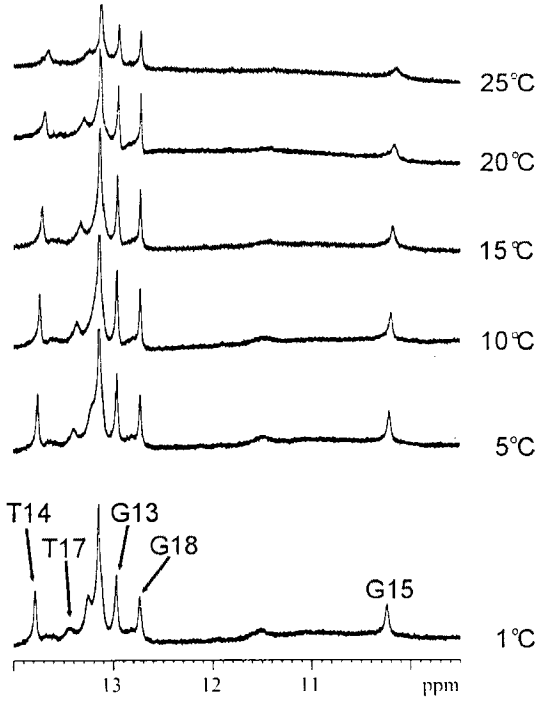

Fig. 4. Expanded NOESY (300-ms mixing time) contour plots of the DW/GA duplex in D_2O buffer at 1°C. (A) A typical region (base to H1' protons) in the sequential NOE connectivity of the Dewar lesion strand and (B) the complementary strand.

to imino NOE interactions of the DW/GA duplex were observed at G2-NH ↔ G18-NH, G18-NH ↔ T17-NH, T14-NH ↔ G13-NH, and G13-NH ↔ G9-NH steps (Figure 2B). The discontinuities, or weakness in the sequential NOEs of imino to imino protons, suggested a significant disturbance in the stacking interaction. The significantly weaker intensity of T17-NH ↔ G18NH than that of the DW/AA duplex (Hwang *et al.*, 1996) indicates that the 5'-side of the Dewar lesion is more destabilized than its 3'-side. The chemical shifts of all imino and the amino protons of all C residues are given in Table 1.

Exchange behavior of the imino protons The temperature-dependent ^{1}H spectra of the imino protons of the DW/GA duplex are presented in Figure 3. Increasing the temperature led to thermal denaturation of the double helical structure with the contaminant line broadening and the eventual disappearance of the imino proton resonances that were formerly involved in hydrogen bonding. One striking feature of the temperature-dependent imino proton spectra in H_2O buffer is the persistence of the G15 imino proton resonance for experiments performed at 1-20°C. These spectra are similar to those of the DW/AA duplex (Hwang *et al.*, 1996). This result indicates that the hydrogen bonding interaction between the 3'-T of the Dewar product and the imino proton of the opposite G15 residue is obviously present, but the stability of the overall helix is not improved by substituting a G for an A opposite the 3'-T site of the Dewar product.

Resonance assignment of the non-exchangeable protons The non-exchangeable proton assignment for the DW/GA duplex was based on an analysis of distance-connectivities in NOESY data sets and bond-connectivities in COSY-type data sets recorded at 1°C. The NOESY spectra were acquired with a variety of mixing times. First, cytosine base proton resonances were identified by their H5 and H6 cross peaks in both NOESY and DQF-COSY spectra. Then, the assignment of base and sugar proton resonances followed from a standard sequential strategy. Expanded portions of a 300-ms NOESY spectrum are shown in Figure 4. These contour plots outlined the sequential intrastrand NOE connectivities between the base H6/H8 and sugar H1' protons. Standard sequential NOE connectivities in the Dewar lesion strand were observed from C1 to A4 and from A7 to C10 (Figure 4A). Saturation of the 5-6 double bond of the T5 base by forming a covalent bond between the T5-C6 and T6-C4 carbons led to the upfield shift of the T5-H6 resonance (4.34 ppm). Photo-conversion of the pyrimidone ring (T6 base) of the (6-4) adduct to the Dewar valence form led to significant upfield shifts of its H6 proton (7.96→4.71 ppm) and methyl resonances (2.33→2.06 ppm). All sequential NOEs of the complementary strand were also observed (Figure 4B). The chemical shifts of non-

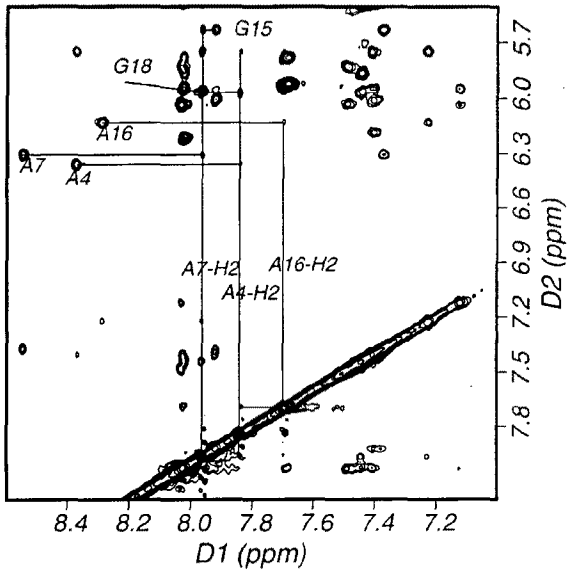

Fig. 5. Expanded NOESY (300-ms mixing time) contour plot of the DW/GA duplex in D_2O buffer at 1°C. NOE interaction between the A-H2 protons and their own and neighboring sugar H1' protons.

exchangeable protons of the DW/GA duplex were listed in Table 1.

The base proton assignments were confirmed in the base to H2'/H2" and base to H3' regions of NOESY contour plot. These regions of the NOESY spectrum were also used for initial assignments of the H2'/H2" and H3' protons. The assignments of the methyl groups were confirmed by the NOE cross peaks between methyl protons and their own, as well as *(n-1)* neighboring base protons. All H2 protons of A4, A7, and A15 residues showed NOE interactions with H1' of their 3'-side and own residue. Also, interstrand NOE cross peaks were observed for A4-H2↔T17-H1', A7-H2↔T14-H1', and A16-H2 ↔T5H1' (Figure 5), which were often associated with a narrow minor group in the bending geometry. This was also the case for the DW/AA duplex (Hwang et al., 1996). Cross peaks involving the H2 resonances are important for constraining the width of the minor groove in order to assess the base-pairing surrounding the Dewar lesion site.

Structure determination The solution structure of the DW/GA duplex was calculated according to the protocols outlined in *Materials and Methods*. A total of 374 distances were restrained in the RMD calculation. These distance restraints consist of 285 interproton distances derived from NOESY data in D_2O buffer, 15 interproton distances obtained from H_2O-NOESYcross peaks, and 74 distances for the Watson-Crick base pairs of the flanking residues. A converged subset of 14 structures refined by the RMD was identified on the basis of low NOE violations and total energies. These structures exhibited pairwise rms deviation (rmsd) values of 1.09Å ± 0.25 for all heavy atoms. Full relaxation matrix refinements of the mean structure yielded a well-converged subset of eight refined structures. Eight superimposed refined structures of the DW/GA duplex are plotted in Figure 6 and exhibit pairwise rmsd values of 0.68Å ± 0.19 for all heavy atoms. Statistical estimations of the DW/GA duplex are shown in Table 2.

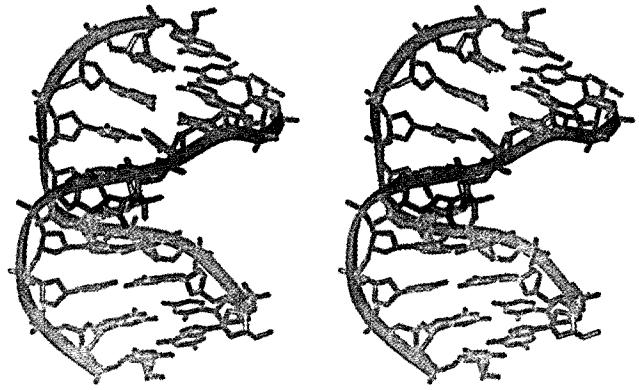

Fig. 6. Solution structure of the DW/GA duplex. Superimposed stereo view of eight intensity-refined structures of the DW/GA duplex.

Table 2. Structure refinement statistics and analysis of DW/GA duplex.

Restrained molecular dynamics	
Number of distance restraints	374
Number of accepted structures	14
Pairwise rmsd (Å)	1.09 ± 0.25
NOE violation energy	92.1 ± 2.5
Number NOE violations:	
Greater than 0.3	0.0 ± 0.0
Greater than 0.2	3.3 ± 0.4
Rmsd from restraints	0.046 ± 0.001
Relaxation matrix refinement	
Number of intensity restraints	738
Number of accepted structures	8
Pairwise rmsd (Å)	0.68 ± 0.19
$R^{1/6}$-factor	0.028 ± 0.000
X-PLOR energies (kcal/mol):	
Total	-853.0 ± 10.7
Bond length	45.1 ± 0.6
Bond angle	178.1 ± 3.5
Dihedral angle	181.5 ± 3.6
Improper angle	28.3 ± 0.2
Hydrogen bond	-193.0 ± 5.1
Van der Waals	-155.6 ± 2.0
Electrostatic	-1115.8 ± 5.7
Relaxation	171.5 ± 10.4
Rmsd from ideal geometry:	
Bond length	0.015 ± 0.000
Bond angle	3.126 ± 0.045
Improper angle	6.692 ± 0.017

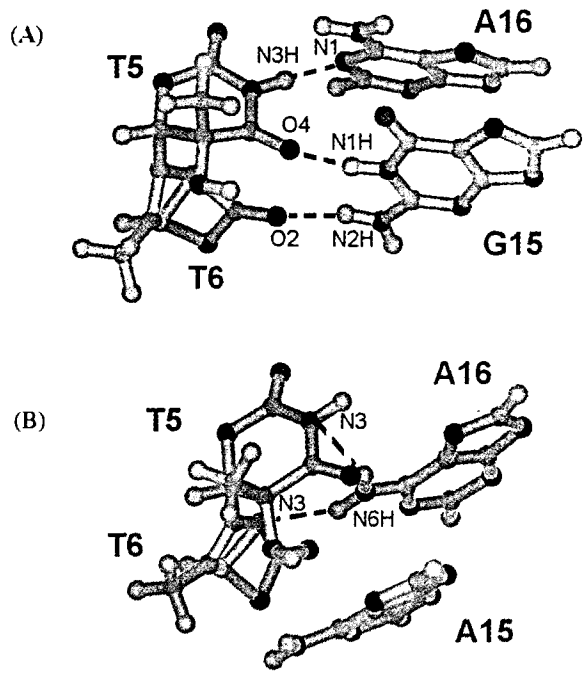

Fig. 7. Ball and stick view of the central four base pairs of the Dewar products in the (A) DW/GA and (B) DW/AA duplexes. The dotted lines indicate the hydrogen bonds determined by the program *INSIGHT II*.

A structural calculation showed that the formation of the Dewar product caused a significant bending (overall bending of 43°) and unwinding (39°) of the DNA helix of the DW/GA duplex. These values are much higher than those of the DW/AA duplex (bending: 21°, unwinding: 16°). This indicates that the insertion of a G residue opposite the 3'-T of the Dewar product distorted the DNA helix more severely than the 3'-T·A base pairing.

Hydrogen bonding feature at the Dewar lesion site The T5·A16 base pair of the Dewar lesion in the DW/GA duplex was shown to deviate from the standard Watson-Crick base pairing geometry. The imino proton of the T5 formed a hydrogen bond to the N1 nitrogen of the opposite A16 residue (Figure 7A). Observations of the T5-imino proton resonance indicate that this unusual hydrogen bonding interaction is significantly weakened by its subsequent structural distortion (Figure 2A). However, the O4 carbonyl oxygen of the T5 residue formed a hydrogen bond, not to the amino proton of the opposite A16, but to the imino proton of the G15 residue (Figure 7A).

The hydrogen bonding feature of the 3'-T (T6) residue of the Dewar product in the DW/GA duplex contrasts with that in the DW/AA duplex. For the DW/GA duplex, the O2 carbonyl oxygen of T6 formed a hydrogen bond with the amino proton of the opposite G15 residue (Figure 7A). However, in the DW/AA duplex, the N3 nitrogen of the T6 residue formed a hydrogen bond with the amino proton of the A16 residue rather than with the opposing A15 residue (Figure 7B).

Table 3. Backbone torsion angles of the photoproduct-containing DNA duplexes

Torsion angles(°)		Duplexes			
		DW/AA	DW/GA	(6-4)/AA	(6-4)/GA
α (*gauche*⁻)	T6	-76.2	-79.7 ± 4.5	149.1	-77.9
	A7	-57.1	-36.7 ± 21.6	-74.0	-63.3
	T14	69.3	-66.0 ± 1.2	-76.1	-76.1
	G13	-66.0	-39.4 ± 3.0	-56.9	-56.9
β (*trans*)	T6	133.6	-173.7 ± 7.6	-146.3	-167.6
	A7	-175.6	133.8 ± 23.9	138.9	175.1
	T14	-143.6	174.1 ± 4.1	159.2	-116.4
	G13	-140.8	128.0 ± 16.7	-179.9	173.6
ε (*trans*)	T6	-13.0	178.7 ± 6.2	-169.6	-173.0
	A7	154.9	-160.4 ± 22.9	-72.9	157.7
	T14	-118.3	-170.8 ± 4.0	-159.8	169.7
	G13	-170.9	-159.8 ± 13.8	-171.7	172.9
ζ (*gauche*⁻)	T6	113.3	-89.0 ± 5.2	-83.0	-95.7
	A7	-85.2	-164.9 ± 27.8	157.0	-78.3
	T14	-93.1	-109.8 ± 16.0	-86.5	-95.8
	G13	-91.4	-171.5 ± 13.4	-110.9	-93.2

Although the 3'-T of the Dewar product can form a hydrogen bond to the opposite G15 residue, this interaction only slightly improved the thermal stability of the overall helix relative to that of the 3'-T·A base pair. These results agree with the thermodynamics studies in which the ΔG° value of a DNA helix, containing a 3'-T·G base pair of the Dewar product, is similar to that of a DNA helix containing a 3'-T·A base pair (Fujiwara & Iwai, 1997).

Backbone conformation The distortions of the backbone conformation caused by the formation of the Dewar product were significantly different in the two duplexes. In the DW/AA duplex, the backbone conformation involving the phosphorous atom between the T6 and A7 residues, which is related to the backbone torsion angles of T6, is significantly distorted (Lee *et al.*, 1998). This backbone distortion reduces the inter-sugar spacing between the T6 and A7 residues, but enlarges the inter-base spacing at the same site. This spacing feature introduces a helical bend, which allows the unusual hydrogen bonding interaction observed between the T6 and A16 residues. Surprisingly, in the DW/GA duplex, the backbone conformation of the A7 and G13 residues of the DW/GA duplex, which involved the two phosphorous atoms between the A7·T14 and C8·G13 base pairs, appeared significantly distorted. These backbone distortions between the A7·T14 and C8·G13 base pairs widened significantly at the major groove of this site. This widening in the DW/GA duplex enables the solvent to interact with the Dewar product bases so that the overall helix becomes destabilized.

Structural basis for mutagenic property of the Dewar product The replicating error frequency of the 3'-T→C transition, which is the most frequent mutation induced by the Dewar lesion, is only 13% in *E. coli* (LeClerc *et al.*, 1991). It has been suggested that the nucleotide substitution mutations, induced by the Dewar lesion during TR, result from physical interactions between a distorted DNA template and an incoming dNTP (LeClerc *et al.*, 1991). The incorporation of a G residue, which forms stable hydrogen bonds with the opposite 3'-T of the Dewar product, did not increase the thermal stability of the overall helix. It also did not restore the distorted backbone conformation of the DNA helix that is caused by the forming of the Dewar lesion. In addition, the helical bending and unwinding angles of the DW/GA duplex were much higher than those of the DW/AA duplex. This demonstrates that no thermal stability, or conformational benefits, are achieved when a G is incorporated instead of an A opposite the 3'-T of the Dewar lesion.

Our previous study concluded that the 3'-T→C transition, induced by the (6-4) adduct, is a misinstructive mutation that is caused by important physical features such as hydrogen bonding, high thermal stability, and no backbone distortion (Lee *et al.*, 1999). However, this structural study of the DW/GA duplex revealed that the 3'-T of the Dewar product does not display more favorable physical interactions when an opposing A residue is replaced by a G residue. This finding indicates that the Dewar product does not exhibit a preference for insertion of a G opposite its 3'-T site during TR. It has been reported that during TR in *E. coli* an A residue is incorporated opposite abasic sites with a frequency of 77% (Jiang & Taylor, 1993). This is in accordance with the A rule, where an A residue is incorporated opposite an abasic lesion with a higher efficiency than is a G residue (Jiang & Taylor, 1993). The G residue opposite the 3'-T of the Dewar product distorts the overall helical configuration more severely than does an A residue. Therefore, we conclude that the incorporation of an A residue opposite the 3'-T of the Dewar lesion is not facilitated by a potential physical interaction, such as hydrogen bonding, but by the incorporation preference of the A residue in a noninstructional manner. These structural properties may thus facilitate the noninstructive incorporation of an A in accordance with the A rule during TR and consequently may lead to the low frequency of 3'-T→C mutations at Dewar lesions.

Acknowledgments This work was supported by the academic research fund of the Ministry of Education, Republic of Korea (Grant 1998-019-D00002).

References

Banerjee, S. K., Christensen, R. B., Lawrence, C. W. and LeClerc, J. E. (1988) Frequency and spectrum of mutations produced by a single *cis-syn* thymine-thymine cyclobutane dimer in a single-strand vector. *Proc. Natl. Acad. Sci. USA* **85**, 8141-8145.

Brash, D. E. (1988) UV mutagenic photoproducts in Escherichia coli and human cells: a molecular genetics perspective on human skin cancer. *Photochem. Photobiol.* **48**, 59-66.

Brünger, A. T. (1992) *X-PLOR* version 3.1 System for X-ray crystallography and NMR (Yale University Press, New Haven, CT).

Cuniasse, P., Sowers, L. C., Eritja, R., Kaplan, B. E., Goodman, M. F., Cognet, J. A., LeBret, M., Guschlbauer, W. and Fazakerley, G. V. (1987) An abasic site in DNA. Solution conformation determined by proton NMR and molecular mechanics calculations. *Nucleic Acids Res.* **15**, 8003-8022.

Fuchs, R. P. P. and Napolitano, R. L. (1998) Inactivation of DNA proofreading obviates the need for SOS induction in frameshift mutagenesis. *Proc. Natl. Acad. Sci. USA* **95**, 13114-13119.

Fujiwara, Y. and Iwai, S. (1997) Thermodynamic studies of the hybridization properties of photolesions in DNA. *Biochemistry* **36**, 1544-1550.

Hwang, G.-S., Kim, J.-K. and Choi, B.-S. (1996) NMR structural studies of DNA decamer duplex containing the Dewar photoproduct of thymidylyl (3'→5') thymidine. Conformational changes of the oligonucleotide duplex by photoconversion of a (6-4) adduct to its Dewar valence isomer. *Eur. J. Biochem.* **235**, 359-365.

Jiang, N. and Taylor, J.-S. (1993) *In vivo* evidence that UV-induced C→T mutations at dipyrimidine sites could result from the replicative bypass of cis-syn cyclobutane dimers or their deamination products. *Biochemistry* **32**, 472-481.

Kalnik, M. W., Chang, C. N., Grollman, A. P. and Patel, D. J. (1988) NMR studies of abasic sites in DNA duplexes: deoxyadenisine stacks into the helix opposite the cyclic analogue of 2-deoxyribose. *Biochemistry* **27**, 924-931.

LeClerc, J. E., Borden, A. and Lawrence, C. W. (1991) The thymine-thymine pyrimidine-pyrimidone (6-4) ultraviolet light photoproduct is highly mutagenic and specifically induces 3' thymine-to-cytosine transitions in *Escherichia coli*. *Proc. Natl. Acad. Sci. USA* **88**, 9685-9689.

Lee, J.-H., Hwang, G.-S. and Choi, B.-S. (1997) NMR studies of the conformation and stability of the 4'-aminomethyl-4,5',8-trimethylpsoralen (AMT) cross-linked DNA octamer duplex, d(GGGTACCC)$_2$. *J. Biochem. Mol. Biol.* **30**, 421-425.

Lee, J.-H., Hwang, G.-S., Kim, J.-K. and Choi, B.-S. (1998) The solution structure of DNA decamer duplex containing the Dewar product of thymidylyl (3'→5') thymidine by NMR and full relaxation matrix refinement. *FEBS Lett.* **428**, 269-274.

Lee, J.-H., Hwang, G.-S. and Choi, B.-S. (1999) Solution structure of a DNA decamer duplex containing the stable 3' T·G base pair of the pyrimidine (6-4) pyrimidone photoproduct [(6-4) adduct]: implication for the highly specific 3' T→C transition of the (6-4) adduct. *Proc. Natl. Acad. Sci. USA* **96**, 6632-6636.

Mitchell, D. L. (1988) The relative cytotoxocity of the (6-4) photoproducts and cyclobutane dimers in mammalian cells. *Photochem. Photobiol.* **48**, 51-57.

Mitchell, D. L. and Nairn, R. S. (1989) The biology of the (6-4) photoproduct. *Photochem. Photobiol.* **49**, 805-819.

Park, J.-Y., Lee, J.-H. and Choi, B.-S. (1998) Structural and dynamic studies of the central segments in the self-complementary decamer DNA duplexes d(ACGTATACGT)$_2$

and d(ACGTTAACGT)$_2$. *J. Biochem. Mol. Biol.* **31**, 89-94.

Pfeifer, G. P. (1997) Formation and processing of UV photoproducts: effects of DNA sequence and chromatin environment. *Photochem. Photobiol.* **65**, 270-283.

Sagher, D. and Strauss, B. S. (1983) Insertion of nucleotides opposite apurinic/apyrimidinic sites in deoxyribonucleic acid during in vitro synthesis: uniqueness of adenine nucleotides. *Biochemistry* **22**, 4518-4526.

Smith, C. A., Wang, M., Jiang, N., Che, L., Zhao, X. and Taylor, J.-S. (1996) Mutation spectra of M13 vectors containing photoproducts of thymidylyl-(3'→5')-thymidine in *Escherichia coli* under SOS conditions. *Biochemistry* **35**, 4146-4154.

Tomer, G., Reuven, N. B. and Livneh, Z. (1998) The β subunit sliding DNA clamp is responsible for unassisted mutagenic translesion replication by DNA polymerase III holoenzyme. *Proc. Natl. Acad. Sci. USA* **95**, 14106-14111.